



HAL
open science

Correlative nonlinear optical microscopy and infrared nanoscopy reveals collagen degradation in altered parchments

Gaël Latour, Laurianne Robinet, Alexandre Dazzi, François Portier, Ariane Deniset-Besseau, Marie-Claire Schanne-Klein

► To cite this version:

Gaël Latour, Laurianne Robinet, Alexandre Dazzi, François Portier, Ariane Deniset-Besseau, et al.. Correlative nonlinear optical microscopy and infrared nanoscopy reveals collagen degradation in altered parchments. *Scientific Reports*, 2016, 6, pp.26344 10.1038/srep26344 . hal-01321012

HAL Id: hal-01321012

<https://hal.sorbonne-universite.fr/hal-01321012v1>

Submitted on 24 May 2016

HAL is a multi-disciplinary open access archive for the deposit and dissemination of scientific research documents, whether they are published or not. The documents may come from teaching and research institutions in France or abroad, or from public or private research centers.

L'archive ouverte pluridisciplinaire **HAL**, est destinée au dépôt et à la diffusion de documents scientifiques de niveau recherche, publiés ou non, émanant des établissements d'enseignement et de recherche français ou étrangers, des laboratoires publics ou privés.



Distributed under a Creative Commons Attribution - NonCommercial - NoDerivatives 4.0 International License

SCIENTIFIC REPORTS



OPEN

Correlative nonlinear optical microscopy and infrared nanoscopy reveals collagen degradation in altered parchments

Received: 30 December 2015

Accepted: 22 April 2016

Published: 19 May 2016

Gaël Latour^{1,*}, Laurianne Robinet^{2,*}, Alexandre Dazzi³, François Portier⁴, Ariane Deniset-Besseau³ & Marie-Claire Schanne-Klein⁵

This paper presents the correlative imaging of collagen denaturation by nonlinear optical microscopy (NLO) and nanoscale infrared (IR) spectroscopy to obtain morphological and chemical information at different length scales. Such multiscale correlated measurements are applied to the investigation of ancient parchments, which are mainly composed of dermal fibrillar collagen. The main issue is to characterize gelatinization, the ultimate and irreversible alteration corresponding to collagen denaturation to gelatin, which may also occur in biological tissues. Key information about collagen and gelatin signatures is obtained in parchments and assessed by characterizing the denaturation of pure collagen reference samples. A new absorbing band is observed near the amide I band in the IR spectra, correlated to the onset of fluorescence signals in NLO images. Meanwhile, a strong decrease is observed in Second Harmonic signals, which are a structural probe of the fibrillar organization of the collagen at the micrometer scale. NLO microscopy therefore appears as a powerful tool to reveal collagen degradation in a non-invasive way. It should provide a relevant method to assess or monitor the condition of collagen-based materials in museum and archival collections and opens avenues for a broad range of applications regarding this widespread biological material.

In museums, libraries and archives, skin is largely present in collections as rawhide, parchment or leather since it has been used for utilitarian purposes, for example in clothes, vessels, writing supports and musical instruments or for decorative purposes. In Western Europe, parchment was the main writing support in the Middle Ages up to the growth of paper production in the 14–15th centuries. Made from an untanned animal skin, it was preserved by liming, scraping and drying the skin under tension¹. Compared to skin, parchment retains only the dermis layer, made mostly of fibrillar collagen (type I).

Among conservators and scientists involved in the preservation of cultural heritage, gelatinization is a term commonly used for parchment alteration. It refers to the collagen denaturation to gelatin, where the triple helix is dissociated. Nevertheless, little is known about the actual transformation process in parchments and the influencing factors. UV radiation, heat or pH can cause perturbations in the bonding within and in-between collagen molecules but this might not be apparent unless water comes into contact with the material. In such a damaged structure, called a “pre-gelatinized” state, the access of water to the collagen molecules is considered to cause the loss of the hydrogen bonds holding the triple helix, resulting in the unfolding of the molecule. The gelatinization resulting from the action of water is accelerated by the additional energy provided by heating^{2,3}. Given that gelatinization is irreversible, the major challenge for the conservation of parchment is to identify collagen in the “pre-gelatinized” state^{2,3} so that suitable treatments or conservation conditions can be selected. To that purpose,

¹Laboratoire Imagerie et Modélisation en Neurobiologie et Cancérologie, Univ. Paris-Sud, Univ. Paris-Diderot, CNRS, Université Paris-Saclay, 91405 Orsay cedex, France. ²Centre de Recherche sur la Conservation, Sorbonne Universités, Muséum national d’Histoire naturelle, Ministère de la Culture et de la Communication, CNRS, 75005 Paris, France. ³Laboratoire de Chimie Physique, Univ. Paris-Sud, CNRS, Université Paris-Saclay, 91405 Orsay cedex, France. ⁴Laboratoire de Chimie de la Matière Condensée de Paris, Sorbonne Universités, UPMC Univ Paris 06, CNRS, Collège de France, 75005 Paris, France. ⁵Laboratoire d’Optique et Biosciences, Ecole Polytechnique, CNRS, INSERM, Université Paris-Saclay, 91128 Palaiseau cedex, France. *These authors contributed equally to this work. Correspondence and requests for materials should be addressed to G.L. (email: gael.latour@u-psud.fr)

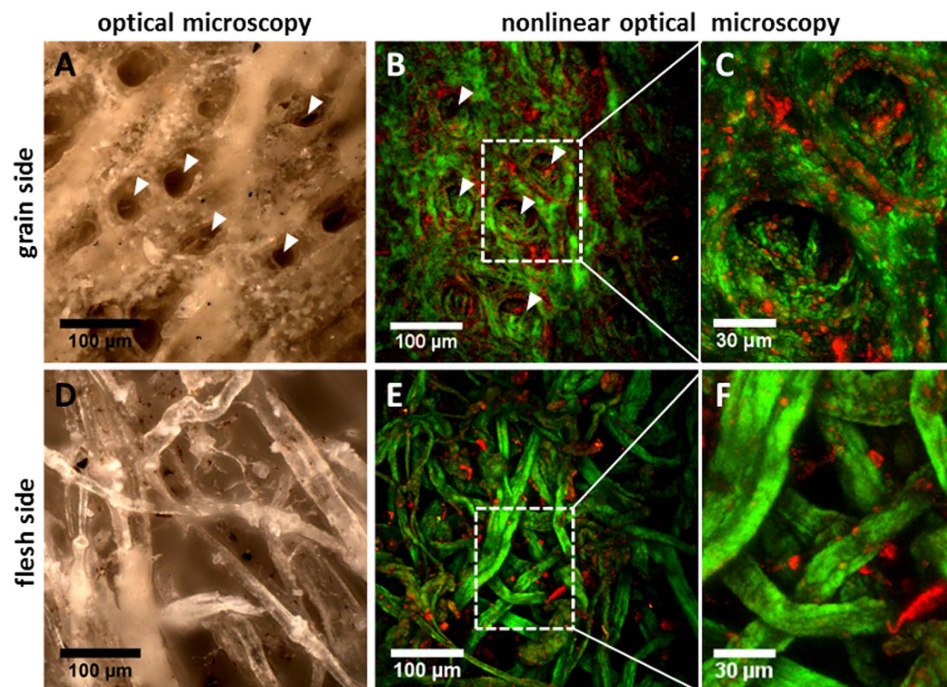


Figure 1. Nonlinear and conventional optical imaging of untanned dry skin. (A,D) Optical microscopy compared to (B,C,E,F) NLO imaging (SHG in green and 2PEF in red) of an untanned skin on (A–C) grain sides where hair follicles are clearly visible (arrows) and (D–F) flesh sides with a more opened structure.

complementary techniques are required to probe alterations at various structural levels including the molecular and fibrillar scales⁴. It is therefore essential to favor the use of non-invasive and non-destructive techniques, especially since sampling may be prohibited due to artefact fragility or preciousness.

Nonlinear optical microscopy (NLO), also called multiphoton microscopy, advantageously provides non-invasive three-dimensional (3D) multimodal imaging of scattering samples with micrometer-scale resolution. This technique can combine two-photon excited fluorescence (2PEF) from exogenous and endogenous fluorophores and second harmonic generation (SHG), which enables the visualization of unstained fibrillar collagen^{5,6}. SHG signals are generated by non-centrosymmetric organizations at molecular scale (collagen triple helix) and amplified by constructive interferences at macromolecular scale (alignment of the collagen molecules to form collagen fibrils)^{6–10}. SHG microscopy is then a structural probe of collagen hierarchical organization, any disruption of which leads to a loss of SHG signals. In biomedical researches, SHG microscopy has emerged as a powerful technique to quantify collagen 3D organization in tissues, in particular in skin dermis^{11,12}. NLO microscopy has recently been applied to the field of cultural heritage^{13–18} but never to examine collagen-based objects.

Nevertheless, this technique cannot resolve nanometer structural features of collagen and the image interpretation may be difficult on materials. Micrometer-scale NLO imaging should therefore be combined with spectroscopic techniques such as infrared (IR) spectroscopy to identify the chemical origin of the morphological changes. IR spectroscopy is used to examine collagen secondary structure in parchment and can be applied to evidence gelatinization¹⁹. However, spectroscopic analysis at the fibers or fibrils scale (~100 nm) is required, which necessitates nanoscale IR spectroscopy (nanoIR), a recent technique combining an Atomic Force Microscope (AFM) with an IR pulsed tunable laser²⁰. This IR nanoscopy allows acquiring chemical mapping and local IR spectra to characterize and image samples at the nanoscale²¹ and has been applied in polymer science and microbiology^{22,23}. It is based on a photothermal effect: when the laser wavelength is tuned on an infrared absorption band of the sample, a photothermal expansion occurs and is directly detected by the tip of the AFM in contact mode.

In this study, we implement correlative NLO imaging and nanoIR characterization of collagen denaturation and we discuss the modification of the nonlinear signals based on the chemical signature. We investigate untanned skin and ancient preserved and altered parchments, as well as pure collagen reference samples to assess collagen and gelatin signatures unambiguously. Finally, we show that NLO imaging provides the local degradation state of ancient parchments as confirmed by chemical measurements using nanoIR.

Results

NLO microscopy of preserved skin: untanned skin versus parchment. SHG and 2PEF signals were collected from both sides of a dried untanned skin that had not been transformed mechanically into a parchment. Compared to conventional optical microscopy, NLO microscopy provides more contrasted specific images (Fig. 1). The collagen displays strong SHG signal due to its dense and non-centrosymmetric fibrillar structure. It also displays a slight 2PEF signal linked to molecule crosslinks²⁴. In the NLO images we clearly distinguish the

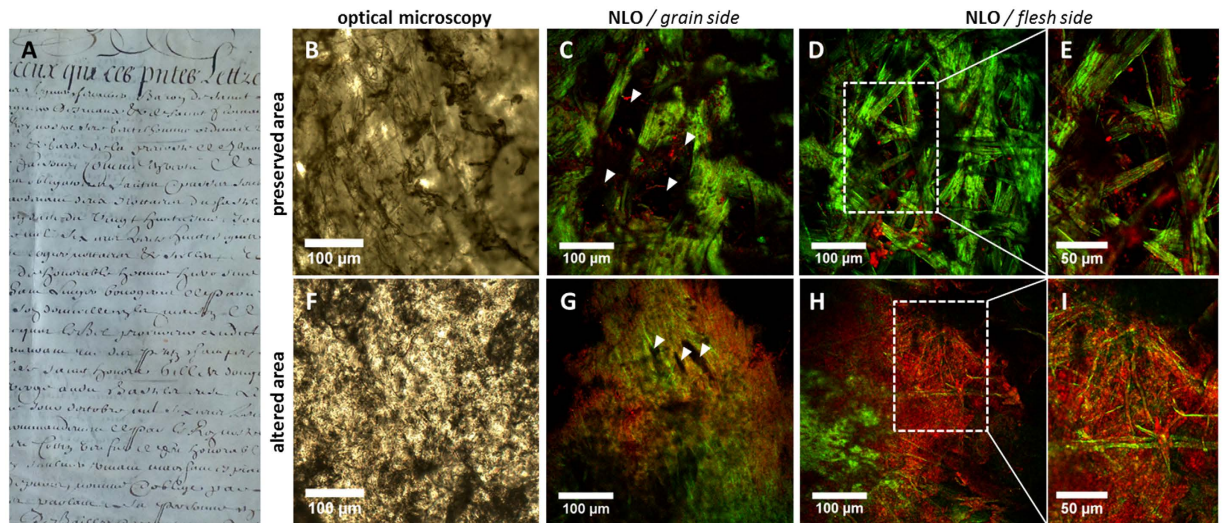


Figure 2. Nonlinear optical microscopy imaging of preserved and altered parchment “1639”. (A) Detail of parchment “1639” (©CRCC, Laurianne Robinet). (B–E) Preserved area of the parchment versus (F–I) artificially altered area by water immersion. (C,G) Grain side with hair follicles (arrows) and (D,E,H,I) flesh side are compared. SHG signals (green) decrease whereas 2PEF signals (red) increase with parchment alteration and collagen fibers organization of preserved parchment (E, zoom in) is replaced by quite homogenous 2PEF signals in altered parchment (I, zoom in).

grain side (hair side) with fine collagen fibers densely packed around hair follicles (arrows in Fig. 1B; Video S1 and Video S2), from the flesh side where thicker fibers or bundles are tangled in a more opened structure (Fig. 1E; Video S3 and Video S4). The NLO images obtained on the grain side of the untanned skin are similar to those collected on *in vivo* skin²⁵. 2PEF images show also localized signals mostly on the edge of the hair holes in the grain side, probably from keratin residues left after removing the hair, and randomly among the fibers in the flesh side, presumably from residues of fat or elastin¹².

In ancient parchments, NLO images reveal a different morphology compared to the untanned skin. SHG images of the ancient parchment “1639” exhibit a strong alignment of the collagen fibers in the image plane, parallel to the skin surface (Fig. 2C–E; Video S5) due to the fibers reorganization involved by the stretching step during manufacturing. Fluorescent clusters randomly spread within the fibers network are also observed. They may again originate from residues of keratin and fat but also from any material accumulated with time within the inner structure of the parchment. The distinction between grain and flesh side in parchment remains possible by the presence of hair follicles (arrows in Fig. 2C,G) and large fibrillary stretched structures respectively, whereas these characteristics are not visible in conventional optical microscopy (Fig. 2B,F).

In the untanned skin, high quality NLO images are collected up to 140 μm deep for the flesh side and down to 100 μm for the grain side, using our acquisition conditions (moderate 0.75 NA air objective and less than 20 mW laser power under the objective, see methods). In a parchment where the thickness is around 200 μm, light can go through the full depth, enabling collection of backward and forward images. Nevertheless, the maximum depth at which we can collect high quality images enabling structural characterization is limited to 70–80 μm, due to the tighter network of fibers that limits light penetration.

NLO microscopy of gelatinized parchments. A sample of parchment “1639” was immersed into water at warm room temperature to obtain artificially “gelatinized” parchment. In conventional optical microscopy the parchment surface has then a gel like appearance (Fig. 2F). In NLO microscopy, SHG signal intensity decreases with a loss of the well identified structures whereas a quite homogenous 2PEF signal appears (Fig. 2G–I). On grain side, hair follicles are still observable but with an enhanced deformation of their round shape (arrows in Fig. 2G). On flesh side, homogenous 2PEF signals dominate even if locally some SHG signal is emitted by sparse collagen fibers (Fig. 2H–I). Due to the more homogenous and dense organization of the altered material depth penetration decreases.

The altered area of a 17th century maritime map made on parchment was also studied (Fig. 3A). Museum conservator and curator considered this area to be “gelatinized” based on the increased translucency and rigidity accompanied by a retraction of the parchment observed macroscopically (inset Fig. 3A). For a more representative investigation, 4 by 3 NLO images were stitched to obtain a 1300 × 1100 μm² field of view (Fig. 3B). The resulting “mosaic” image of this “gelatinized” area shows similar results to those on the artificially altered parchment with a decrease or disappearance of the SHG signal and an increase of the 2PEF signal. Depth profiles of the 2PEF and SHG signal intensities confirm the strong correlation between SHG and 2PEF signal variations (Fig. 3C). Some SHG signal still remained locally but with a more homogenous distribution (Fig. 3D,F). In the altered areas, the 2PEF signal is homogenous except for some bundles with only fluorescent signals (see arrows in Fig. 3B). Given that SHG signals are specific for fibrillary structures, these NLO microscopy results indicate that

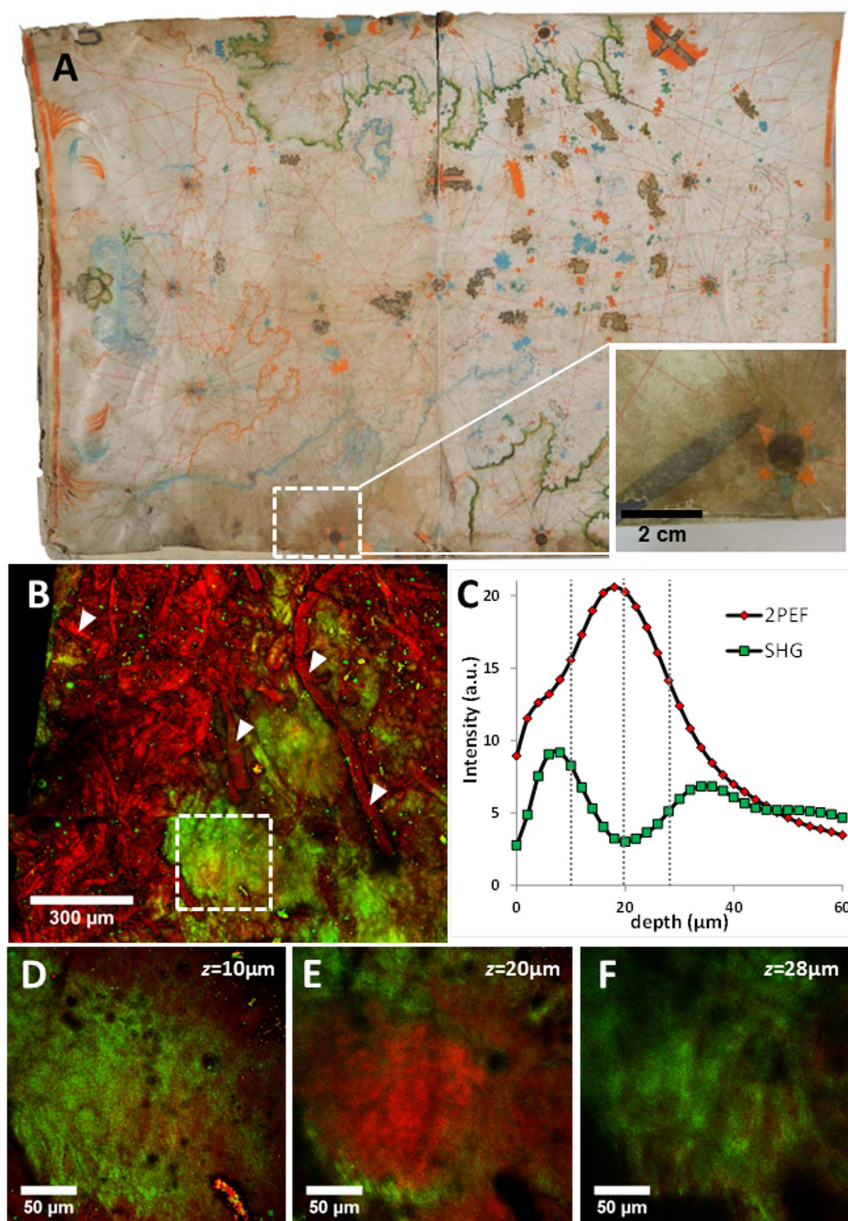


Figure 3. Nonlinear optical microscopy imaging of a 17th century Maritime map. (A) Navigation map of the Aegean sea, 17th century illuminated parchment, $58.8 \times 39 \text{ cm}^2$ (©INP, Ghyslain Vanneste). Inset: zoomed view of the gelatinized area. (B) NLO imaging of the gelatinized area with some fluorescent bundles (arrows) (mosaic, field of view $1300 \times 1100 \mu\text{m}^2$, pixel size $0.8 \mu\text{m}$). (C) Average intensity depth profile over the white square area in B and (D–F) zoomed NLO images at different depths (10, 20 and $28 \mu\text{m}$ deep).

the gelatinization process induces the loss of fibrillar organization of collagen and the formation of an unstructured material exhibiting a higher fluorescence, with several intermediate degradation stages. The material has changed from an opened fibrillar structure that scatters light to a compact structure at the microscopic scale, which explains its macroscopic optical modifications as an increased transparency and its brittleness. Lastly, the SHG signal from particles of a few micrometers in diameter is also observed (Fig. 3B). This SHG signal is likely to come from calcium carbonate, which displays a strong SHG signal due to its surface anisotropy (Supplementary Fig. S1)²⁶. This material is formed in parchment during manufacturing, mostly by reaction of the lime on the skin with carbon dioxide (CO_2) of the air or occasionally by application of chalk on the surface.

Multiscale and NLO-nanoIR correlative imaging of preserved and altered parchment. Correlative NLO microscopy and IR nanoscopy was implemented to identify the chemical compounds associated with the modified structure observed in the NLO images of the degraded parchment. Fibrillar collagen shows different absorption bands in the mid IR region (4000 cm^{-1} to 400 cm^{-1}), notably the amide I band ($\text{C}=\text{O}$ stretching vibration $1680\text{--}1590 \text{ cm}^{-1}$) and the amide II band (mostly N-H deformation $1590\text{--}1510 \text{ cm}^{-1}$) specific for

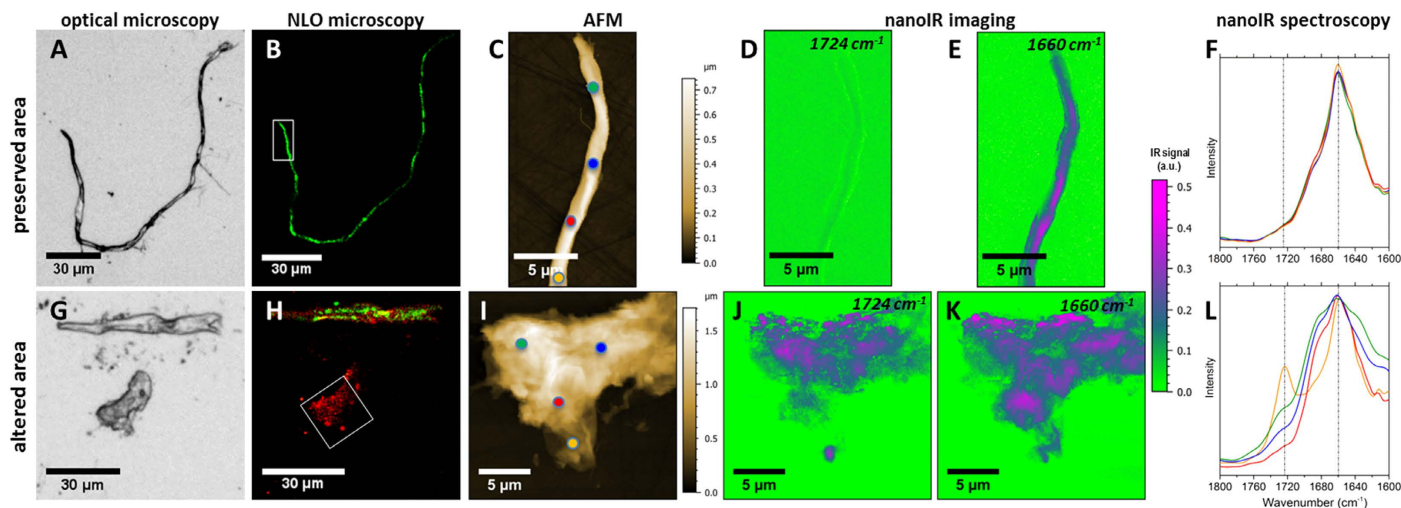


Figure 4. Correlative imaging of sample scrap from preserved and altered parchment “1639”. Correlative imaging and IR nanoscopy characterization from (A–E) preserved and (G–K) altered parchment: (A,G) optical microscopy, (B,H) NLO microscopy, (C,I) AFM topography, nanoIR mapping at (D,J) 1724 cm^{-1} and (E,K) 1660 cm^{-1} . (F,L) NanoIR spectra recorded between 1600 and 1800 cm^{-1} from local areas (colored points in AFM images) in the preserved and altered samples. The carbonyl vibration at 1724 cm^{-1} clearly appears in the nanoIR spectra from the altered parchments and (J) nanoIR mapping at this wavenumber exhibits strong signals on the contrary to (D) the mapping from the preserved one.

peptide vibrations. The position of the carbonyl band (amide I) strongly depends on the environment and the substituent of the nitrogen atom for example carboxylic acid ($1740\text{--}1700\text{ cm}^{-1}$) or ester ($1750\text{--}1730\text{ cm}^{-1}$) group.

In parchment “1639”, AFM topography shows that mostly fibers are present in the preserved areas for which only SHG was detected (Fig. 4A–C), whilst clusters are present in the artificially altered area giving off only 2PEF signal with hot spots sparsely dispersed (Fig. 4G–I). Beyond these morphological differences, local nanoIR spectra between 1800 and 1450 cm^{-1} provided different signatures. The IR spectra acquired all along the fiber consistently display the two bands associated with Amide I at 1660 cm^{-1} (Fig. 4F) and Amide II at 1548 cm^{-1} . In comparison, the spectra acquired in the clusters show a broadening of the amide bands (Fig. 4L). The broadening may be induced by a shift of the bands either following a degradation of the collagen or a humidity variation²⁷. Most interestingly, the occurrence of a new carbonyl vibration band around 1724 cm^{-1} different from the carbonyl of the amide group is observed in the degraded regions of the sample. To assess the specificity of this vibration band for denatured collagen, IR mappings of the same areas were collected at 1660 cm^{-1} , which is representative of the amide I band (Fig. 4E,K), and at 1724 cm^{-1} (Fig. 4D,J). We obtained an excellent correlation between nanoIR mappings and NLO images, confirming that the presence of the new carbonyl band in vibrational spectra is correlated with the appearance of fluorescence signals. As this new carbonyl band is not clearly associated to a functional group we will call it “gel-carbonyl” band in this report to discriminate it from the amide I band.

To support this observation, reference samples of pure fibrillar collagen and of gelatin prepared in water were measured (Fig. 5). In the optical and AFM topography images, the reference samples display different morphology with dispersed fibers for the collagen and isolated clusters of approximately $10\text{--}40\text{ }\mu\text{m}$ in size for the gelatin. As expected, the images obtained by NLO microscopy on the fibrillar collagen display strong SHG signal with little 2PEF, whilst the isolated clusters of the gelatin exhibit strong fluorescence without any SHG signal. NanoIR spectra collected between 1800 and 1450 cm^{-1} show a broadening of the amide bands in the gelatin compared to the fibrillar collagen. Moreover, the presence of a particularly intense carbonyl vibration band centered at 1738 cm^{-1} in all the gelatin spectra is observed, suggesting that the gel-carbonyl band is characteristic of the gelatin formation. These results confirm that the modifications of NLO signals with quite high fluorescence in altered parchments are associated with the formation of gelatin and the appearance of a new chemical signature.

Finally, the correlative approach by NLO microscopy and IR nanoscopy was applied to a tiny scrap originating from a “gelatinized” area of the maritime map (Fig. 6). In the NLO images, we mostly observed clusters where local fluorescent hot spots were detected. Single infrared spectra collected between 1800 and 1600 cm^{-1} on the clusters show the amide I bands at 1670 cm^{-1} as well as the gel-carbonyl band at 1724 cm^{-1} specific from gelatinized collagen (Supplementary Fig. S2). NanoIR mapping at 1724 cm^{-1} on different clusters shows a strong correlation between fluorescent hot spots and the gel-carbonyl band (Fig. 6B,E). However, IR mapping at 1660 cm^{-1} is not correlated with SHG imaging (Fig. 6C,F). This means that fluorescence is associated with the appearance of the gel-carbonyl band whereas SHG imaging reveals specifically the preserved collagen which is organized fibrillarly. 2PEF signals associated with the absence of SHG signals thus enable micrometer scale mapping of the gelatinized areas and could be used to precisely locate early and localized alteration areas.

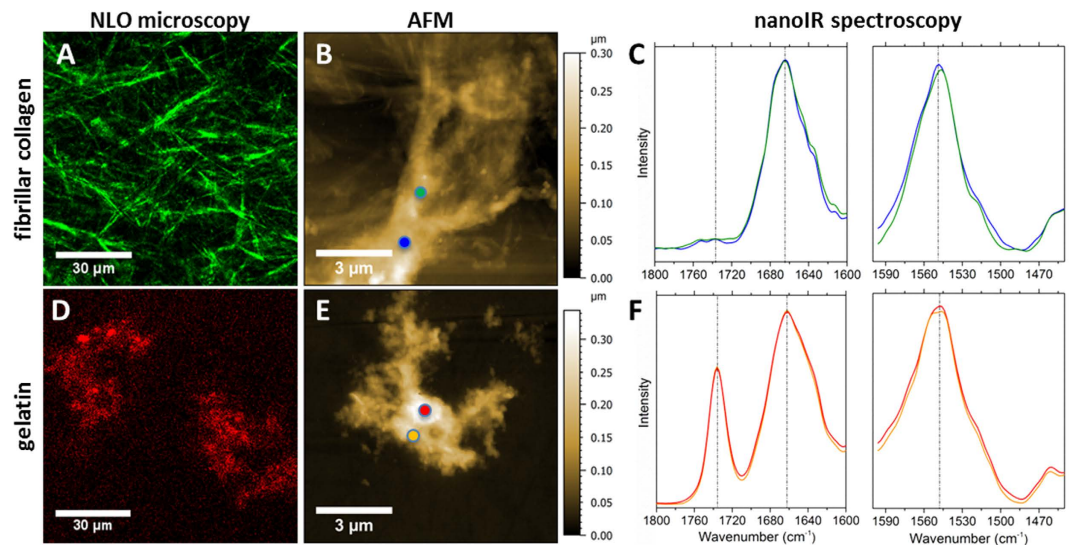


Figure 5. Comparative imaging and IR nanoscopy characterization of collagen references. (A–C) Fibrillar collagen and (D–F) denatured collagen observed by NLO microscopy from (A) fibrillar collagen and (D) gelatin and (B,E) AFM topography. (C,F) Infrared spectra from local areas highlighted with the colored point in AFM images, recorded between 1450 and 1800 cm^{-1} , exhibit amide I ($\sim 1660 \text{ cm}^{-1}$) and amide II ($\sim 1550 \text{ cm}^{-1}$) bands and (F) the appearance of a carbonyl vibration (at 1738 cm^{-1}) for the denatured collagen.

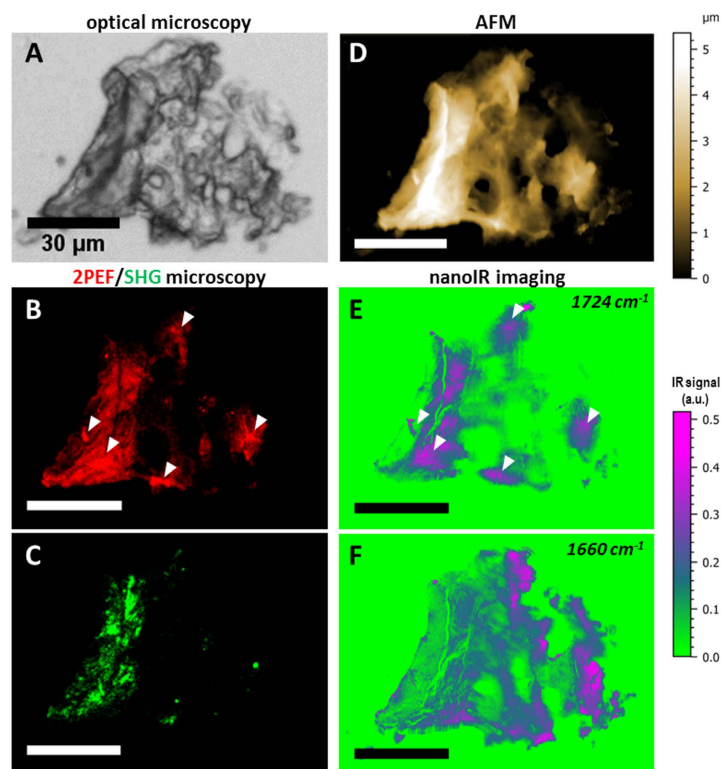


Figure 6. Correlative imaging of Maritime map sample scrap. Correlative (A) optical microscopy, (B) 2PEF microscopy, (C) SHG microscopy, (D) AFM topography, nanoIR mapping at (E) 1724 cm^{-1} and (F) 1660 cm^{-1} . Arrows in the 2PEF microscopy image (B) show hot fluorescent areas in the cluster and are correlated with the nanoIR mapping at 1724 cm^{-1} , corresponding to the gel-carbonyl band.

Discussion

In this work, we present the first application of NLO microscopy and IR nanoscopy to the study of ancient parchments and their alteration, giving a new insight into the understanding of collagen degradation by coupling nonlinear optical signals and chemical information.

The structural specificity of the SHG signal to fibrillar collagen allows collecting non-invasively well-contrasted 3D images of the fiber organization in skin-based materials. This technique clearly evidences structural differences linked to parchment orientation, manufacturing or alteration. Our data show that the parchment alteration is associated with a decrease or loss of the SHG signal and a joint increase in the 2PEF signal. The structural organization is also strongly affected with the collagen fibers being disassembled and the formation of an amorphous and compact material providing a strong homogenous fluorescence signal.

The origin of these modifications in the NLO images was identified using IR nanoscopy. Comparison of pure gelatin and collagen reference samples prepared from the same collagen batch showed that the gelatin exhibits a new band at 1738 cm^{-1} . A similar band was observed at 1724 cm^{-1} in the degraded parchment. This carbonyl vibration band is likely to come from the formation of acidic species which may have different origins. In parchment, the onset of a weak band between 1750 and 1700 cm^{-1} in the IR spectra has been reported for different alteration processes: acidification, hydrolysis and oxidation²⁸. In the case of the collagen denaturation into gelatin, the most likely mechanisms are acidification, causing the protonation of the side chain on the carboxyl group of glutamic and aspartic acids, and the hydrolysis of collagen leading to the formation of COOH terminal and NH_3^+ . Hydrogen bonding affects the position of this band, which may explain the difference in band position observed between degraded parchment and gelatin samples²⁹. The strong intensity of this carbonyl band in our data might be explained by the fact that IR nanoscopy is a very local analytical technique.

The nanometer scale spatial resolution provided by IR nanoscopy coupled to the imaging approach could be of great interest for the field of cultural heritage. It would allow the characterization of the distribution of compounds at low concentrations in heterogeneous material, such as thin layers in a stratigraphy or degradation products in a mixed media. Although the technique is invasive, the amount of sample required is extremely low and might allow the study of collections previously inaccessible. For parchment, IR nanoscopy allows collecting measurement directly on individual collagen fibers ($\sim 1\text{--}5\text{ }\mu\text{m}$) or fibrils ($\sim 100\text{ nm}$), not accessible with conventional or even synchrotron-based IR microscopy, which have spatial resolutions around 50 and $10\text{ }\mu\text{m}$ respectively. Such studies might therefore reveal heterogeneity in the degradation at the fiber scale. In addition, the nanoIR spectra are not affected by the strong absorbance of the carbonate or sulfate compounds found in parchments (for instance calcium carbonate originating from liming), whilst these signals generally interfere with the amides bands in the spectra collected on conventional IR instrument and render data interpretation difficult. Finally, while IR illumination from below the sample limits nanoIR measurements to samples with thickness below $1\text{ }\mu\text{m}$, new commercial systems where samples can be illuminated from above might overcome that constraint and allow thicker samples to be examined.

This IR nanoscopy technique was combined with NLO microscopy in a correlative approach in order to add chemical information to SHG-2PEF images. The SHG signal construction is related to the hierarchical organization of fibrillar collagen. The loss of signal observed in degraded regions of the parchment is therefore caused by any modification or disruption in the collagen assembly, as confirmed by the AFM topography image and the modifications of the IR spectra. The 2PEF images are strongly correlated with the IR imaging at 1724 cm^{-1} , which was proved to be specific for gelatin formation using reference samples. Whilst the relationship between the 2PEF increase and the denaturation of collagen to gelatin is not perfectly clear, this correlation proves that 2PEF signals probe collagen denaturation in parchments. The correlation of NLO and IR techniques at micrometer and nanometer scales therefore offers a multiscale investigation of materials and gives clues about collagen degradation at both molecular and macromolecular scales.

Finally, our study demonstrates that NLO microscopy has a high potential for the study of parchments. Because of the non-invasivity and the rapidity of the measurements, it is possible to work directly on any ancient artefacts, and examine several regions, mapping representative fields of view of a few square millimeters with sub-micrometer spatial resolution, which is crucial to take into account the heterogeneity of parchment. Such development should help identify parchment most at risk in the museum or archive collections and take suitable conservation measures. It may also help visualize the hair follicles organization for animal species identification. Further study could investigate for example the response of the parchment to different environmental conditions (eg. humidity) or conservation treatment but also to mechanical constraints in dynamic mode directly under the microscope³⁰. By taking advantage of 2PEF spectroscopy, complementary 3D information about the materials used at the surface (pigments, dyes)¹⁵ or retained within the parchment¹² could also be obtained. All these applications would benefit from improved penetration depth using adaptive optics to correct for optical aberrations induced by index mismatch between the parchment and the air objective lens³¹. Similarly, they would be strongly facilitated by the development of portable or transportable instrumentation, as already in progress for biomedical applications.

In conclusion, NLO microscopy provides non-invasive characterization of parchment alteration. The follow-up of the SHG signals appears as a powerful tool to detect early steps of collagen degradation, assessed by the correlative approach with IR nanoscopy that gives clues about the local chemical modifications. The parallels made between the *in vivo* skin, the purified collagen/gelatin reference and the parchment alteration suggests that transposition can be made between research studies in the biomedical and the heritage fields, opening this correlative approach to broader fields of application.

Methods

Collagen references, skin and ancient parchments. *Untanned skin.* An untanned dried calf skin prepared within the European project STEP³².

Parchment "1639". A parchment (sheep or goat) of unknown origin possibly dating from the 17th century as the date 1639 is written on the document. A fragment of this parchment was artificially altered by immersion in distilled water for two days at room temperature in summer (temperature $\sim 30\text{--}35\text{ }^\circ\text{C}$) causing partial denaturation.

Maritime map. Illuminated parchment (sheep) representing the Aegean sea, dated from 17th century, belonging to the National Maritime Museum in Paris, France (Fig. 3A). The “gelatinization” of the lower part of the parchment was caused by water damage during a flood³³. During a restoration, a micro-sample was taken from the suspected gelatinized area for scientific investigations.

Collagen/gelatin references. Type I collagen was purified from rat tail tendon and solubilized in 500 mM acetic acid³⁴. Concentration was determined by hydroxyproline titration as 2.5 mg/mL. To obtain the collagen reference sample, a solution was fibrillated under ammonia vapor overnight, and the resulting collagen gel was washed several times in distilled water. The gelatin reference sample was obtained from the same collagen acid solution after thermal denaturation at 45 °C during 30 min. The denaturation was checked by circular dichroism using a JASCO J-810 spectropolarimeter (Supplementary Material and Supplementary Fig. S3)³⁵. This acid solution of denaturated collagen was then dialyzed again in distilled water to obtain gelatin in water. Two different batches of such samples were obtained and used as reference samples.

Conventional optical microscopy. Microscope Zeiss Imager D2m. Optical images were collected in transmission with an air objective (20×, 0.5 NA).

Nonlinear optical microscopy. A custom-built upright microscope based on a femtosecond Ti:Sa laser (Mai Tai, SpectraPhysics) tuned to 860 nm was used as previously described¹⁵. A high numerical aperture air objective (20×, NA 0.75, Olympus) was used for noncontact imaging and 0.7 μm μm lateral by 4 μm axial resolutions near the sample surface were achieved with 860 nm excitation. Simultaneous 2PEF (GG400 high-pass filter, Schott) and SHG (427/10 interferential filter, Semrock) signals were epi-detected by using photon-counting photomultiplier tubes (P25PC, Electron Tubes). 2PEF and SHG signals are represented in false colors, respectively red and green. The acquisition pixel rate was 200 kHz that corresponds to around one frame per second for 640 × 640 pixel wide images (480 × 480 μm² with 0.8 μm pixel size). Laser power at the objective focus was 8 to 20 mW, without any observable damage in the studied samples.

Several images were acquired in different regions of every sample: 5 images in untanned skin, 13 and 20 images in respectively preserved and altered areas of “1639” parchment. A large image of size 1.3 × 1.1 mm² was acquired in the maritime map by stitching 4 × 3 images at sequential positions.

Nanoscale IR spectroscopy. A commercial system from Anasys Instruments (“nanoIR”, Anasys Instrument) was used for nanoscale IR spectroscopy. Resolution and performances have been previously detailed²³. Shortly, IR illumination was produced by an OPO with 10 ns pulses tunable between 4000 and 1000 cm⁻¹ at 1 kHz repetition rate. The spot diameter was around 50 μm in the 1800 to 1500 cm⁻¹ range, and the power was set at 3 μJ per pulse. Although the laser spot was large, the sharp AFM tip served as a near-field detector by locally detecting the small thermal expansion resulting from light absorption in the sample thus conferring high lateral resolution to the measurements. The resulting spatial resolution for IR mapping has been shown to be between 50 and 100 nm depending on the response of the absorbing object²³.

All IR mappings and spectra were normalized to the incident power. IR mappings were acquired at a scan rate of 0.2 Hz and averaged on 8 pulses. Local spectra were collected using a 2 cm⁻¹ step scan and averaging each data point on 256 pulses. Furthermore, three spectra acquired at the same location were averaged. The spectral resolution was estimated as 8 cm⁻¹ (OPO pulse width). Topographic images were acquired in contact mode with cantilevers of 0.03 N/m (HQ:CSC/AIBS, μmasch).

We verified that no damage was induced within the samples after the acquisition of spectra or IR mappings by controlling the morphology of the sample in topographic images and by checking the stability and reproducibility of the IR spectra. Accordingly, the temperature increase inside the excited area has been estimated to be less than 1 K³⁶.

Correlative imaging. Measurements were carried out on minute scrap taken on the parchment samples, detached in a drop of distilled water, deposited on a CaF₂ windows and left to air dry. This CaF₂ window (200 μm thick and 10 mm of diameter) advantageously exhibits transparency to IR radiation and provides neither SHG nor 2PEF signals. Paraffin oil was used in between this window and the CaF₂ prism in IR nanoscopy to ensure a good optical contact and avoid evanescent waves in the air gap. Correlative imaging was then obtained through successive steps, going from larger to smaller scale: (i) conventional white light optical images of the entire CaF₂ window surface were recorded (10 × 10 mm²); (ii) NLO images (500 × 500 μm²) were acquired on the smallest features to identify 2PEF and SHG signals from different areas (fibrils or clusters); (iii) AFM topography images were obtained in smaller regions (25 × 25 μm²) before to record local nanoIR spectra and nanoIR mappings at 1660 and 1724 cm⁻¹.

Correlative images were acquired in 3 regions of interest of a tiny scrap from the “1639” parchment, in 5 regions of interest of a tiny scrap from the maritime map, and in 8 regions of interest of the reference samples (4 gelatin and 4 fibrillar collagen, from the 2 batches).

References

1. Kite, M. & Thompson, R. *Conservation of leather and related materials*. Elsevier Butterworth-Heinemann, Amsterdam, (2006).
2. Gonzalez, L. G. & Wess, T. J. The effects of hydration on the collagen and gelatin phases within parchment artefacts. *Heritage Science* **1**, 14 (2013).
3. Gonzalez, L. & Wess, T. The importance of understanding the terminology of collagen and gelatin in the study of parchment. *Journal of the Institute of Conservation* **36**(2), 104–108 (2013).

4. Larsen, R. *et al.* Preprints of ICOM Committee for Conservation 14th Triennial Meeting, The Hague, 978-1844072538, 199–208. (2005).
5. Zipfel, W. R. *et al.* Live tissue intrinsic emission microscopy using multiphoton-excited native fluorescence and second harmonic generation. *Proc. Natl. Acad. Sci. USA* **100**(12), 7075–7080 (2003).
6. Campagnola, P. J. & Loew, L. M. Second-harmonic imaging microscopy for visualizing biomolecular arrays in cells, tissues, and organisms. *Nat. Biotechnol.* **21**(11), 1356–1360 (2003).
7. Tuer, A. E. *et al.* Nonlinear optical properties of type I collagen fibers studied by polarization dependent second harmonic generation microscopy. *J. Phys. Chem. B* **115**(44), 12759–12769 (2011).
8. Duboisset, J. *et al.* A bottom-up approach to build the hyperpolarizability of peptides and proteins from their amino acids. *J. Phys. Chem. B* **117**(34), 9877–9881 (2013).
9. Brown, C. P. *et al.* Imaging and modeling collagen architecture from the nano to micro scale. *Biomed. Opt. Express* **5**(1), 233–243, Jan (2014).
10. Bancelin, S. *et al.* Determination of collagen fibril size via absolute measurements of second-harmonic generation signals. *Nat. Commun.* **5**, 4920 (2014).
11. Masters, B. R., So, P. T. & Gratton, E. Multiphoton excitation fluorescence microscopy and spectroscopy of *in vivo* human skin. *Biophys. J.* **72**, 2405–2412 (1997).
12. Pena, A., Strupler, M., Boulesteix, T. & Schanne-Klein, M.-C. Spectroscopic analysis of keratin endogenous signal for skin multiphoton microscopy. *Opt. Express* **13**(16), 6268–6274 (2005).
13. Cormack, I. G. *et al.* Lost writing uncovered by laser two-photon fluorescence provides a *terminus post quem* for roman colonization of *Hispania Citerior*. *J. Archaeol. Sci.* **34**(10), 1594–1600 (2007).
14. Filippidis, G., Gualda, E. J., Melessanaki, K. & Fotakis, C. Nonlinear imaging microscopy techniques as diagnostic tools for art conservation studies. *Opt. Lett.* **33**(3), 240–242 (2008).
15. Latour, G., Echard, J.-P., Didier, M. & Schanne-Klein, M.-C. *In situ* 3D characterization of historical coatings and wood using multimodal nonlinear optical microscopy. *Opt. Express* **20**(22), 24623–24635 (2012).
16. Samineni, P., deCruz, A., Villafana, T. E., Warren, W. S. & Fischer, M. C. Pump-probe imaging of historical pigments used in paintings. *Opt. Lett.* **37**(8), 1310–1312 (2012).
17. Villafana, T. E. *et al.* Femtosecond pump-probe microscopy generates virtual cross-sections in historic artwork. *Proc. Natl. Acad. Sci. USA* **111**(5), 1708–1713 (2014).
18. Filippidis, G., Tserevelakis, G., Selimis, A. & Fotakis, C. Nonlinear imaging techniques as non-destructive, high-resolution diagnostic tools for cultural heritage studies. *Appl. Phys. A* **118**(2), 417–423 (2014).
19. Gonzalez, L., Wade, M., Bell, N., Thomas, K. & Wess, T. Using attenuated total reflection fourier transform infrared spectroscopy (ATR FT-IR) to study the molecular conformation of parchment artifacts in different macroscopic states. *Appl. Spectrosc.* **67**(2), 158–162 (2013).
20. Dazzi, A. *et al.* AFM-IR: Combining atomic force microscopy and infrared spectroscopy for nanoscale chemical characterization. *Appl. Spectrosc.* **66**(12), 1365–1384 (2012).
21. Felts, J. R. *et al.* Atomic force microscope infrared spectroscopy on 15 nm scale polymer nanostructures. *Rev. Sci. Instrum.* **84**(2), 023709 (2013).
22. Deniset-Besseau, A., Prater, C. B., Virolle, M.-J. & Dazzi, A. Monitoring triacylglycerols accumulation by atomic force microscopy based infrared spectroscopy in streptomyces species for biodiesel applications. *J. Phys. Chem. Lett.* **5**(4), 654–658 (2014).
23. Centrone, A. Infrared imaging and spectroscopy beyond the diffraction limit. *Annu. Rev. Anal. Chem.* **8**(1), 101–126 (2015).
24. Richards-Kortum, R. & Sevick-Muraca, E. Quantitative spectroscopy for tissue diagnosis. *Annu. Rev. Phys. Chem.* **47**, 555–606 (1996).
25. Koenig, K. & Riemann, I. High-resolution multiphoton tomography of human skin with subcellular spatial resolution and picosecond time resolution. *J. Biomed. Opt.* **8**(3), 432–439 (2003).
26. Andersson, S. K., Schanne-Klein, M. C. & Hache, F. Symmetry and phase determination of second-harmonic reflection from calcite surfaces. *Phys. Rev. B* **59**, 3210–3217 (1999).
27. Brodsky-Doyle, B., Bendit, E. G. & Blout, E. R. Infrared spectroscopy of collagen and collagen-like polypeptides. *Biopolymers* **14**(5), 937–957 (1975).
28. Kennedy, G. J. & Wess, T. J. The structure of collagen with parchment - a review. *Restaurator* **24**(2), 61–80 (2003).
29. Barth, A. The infrared absorption of amino acid side chains. *Prog. Biophys. Mol. Biol.* **74**, 141–173 (2000).
30. Gusachenko, I., Tran, V., Goulam-Houssen, Y., Allain, J.-M. & Schanne-Klein, M.-C. Polarization-resolved second harmonic generation in tendon upon mechanical stretching. *Biophys. J.* **102**(9), 2220–2229 (2012).
31. Zeng, J., Mahou, P., Schanne-Klein, M.-C., Beaufrepaire, E. & Débarre, D. 3D resolved mapping of optical aberrations in thick tissues. *Biomed. Opt. Express* **3**(8), 1898–1913 (2012).
32. Larsen, R., Vest, M. & Calnan, C. STEP leather project, European commission DG XII, research report No. 1. (1994).
33. Duqueyroy, N., Robinet, L. & Barbe, C. Expandable polyester hinges for parchment mounting. performance in fluctuating environmental conditions. *Journal of Paper Conservation* **16**, 18–28 (2015).
34. Gobeaux, F. *et al.* Fibrillogenesis in dense collagen solutions: A physicochemical study. *J. Mol. Biol.* **376**(5), 1509–1522 (2008).
35. Fasman, G. D. *Circular dichroism and the conformational analysis of biomolecules*. Springer, New York, (2010).
36. Lu, F. & Belkin, M. A. Infrared absorption nano-spectroscopy using sample photoexpansion induced by tunable quantum cascade lasers. *Opt. Express* **19**(21), 19942–19947 (2011).

Acknowledgements

The authors thank Carole Aimé, Gervaise Mosser, Thibaud Coradin, Bertrand Lavedrine and Claire Teulon for critical scientific discussion, David Peggie for critical reading of the manuscript and Nadège Duqueyroy and Marjolaine Mourot for providing access to the maritime map. This work was partly supported by Agence Nationale de la Recherche (contracts ANR-10-INBS-04 France BioImaging and ANR-11-EQPX-0029 Morphoscope2).

Author Contributions

G.L., L.R. and M.C.S.K. designed the research project. G.L. and L.R. designed the N.L.O. experiments and acquired and processed the N.L.O. data. A.D. and A.D.B. designed the nanoIR experiments and acquired and processed the nanoIR data. F.P. designed and prepared the model samples. G.L., L.R., A.D., A.D.B. and M.C.S.K. designed the protocols for correlative measurements. All authors discussed the results and commented about the manuscript. G.L., L.R. and A.D.B. prepared the figures and the methods for the manuscript. G.L., L.R. and M.C.S.K. wrote the manuscript.

Additional Information

Supplementary information accompanies this paper at <http://www.nature.com/srep>

Competing financial interests: The authors declare no competing financial interests.

How to cite this article: Latour, G. *et al.* Correlative nonlinear optical microscopy and infrared nanoscopy reveals collagen degradation in altered parchments. *Sci. Rep.* **6**, 26344; doi: 10.1038/srep26344 (2016).



This work is licensed under a Creative Commons Attribution-NonCommercial-NoDerivs 4.0 International License. The images or other third party material in this article are included in the article's Creative Commons license, unless indicated otherwise in the credit line; if the material is not included under the Creative Commons license, users will need to obtain permission from the license holder to reproduce the material. To view a copy of this license, visit <http://creativecommons.org/licenses/by-nc-nd/4.0/>